Coherent and dislocated three-dimensional islands of $In_xGa_{1-x}N$ self-assembled on GaN(0001) during molecular-beam epitaxy

Y. Liu, Y. G. Cao, H. S. Wu, and M. H. Xie*

Physics Department and the HKU-CAS Joint Laboratory on New Materials, The University of Hong Kong, Pokfulam Road, Hong Kong, China

S. Y. Tong

Department of Applied Physics and Materials Science, City University of Hong Kong, Tat Chee Avenue, Kowloon, Hong Kong

Molecular-beam epitaxy of $In_xGa_{1-x}N$ alloy on GaN(0001) is investigated by scanning tunneling microscopy. The Stranski-Krastanov mode of growth of the alloy is followed, where the newly nucleated three-dimensional islands are initially coherent to the underlying GaN and the wetting layer, but then become dislocated when grown bigger than about 20 nm in the lateral dimension. Two types of islands show different shapes, where the coherent ones are cone shaped and the dislocated ones are pillar like, having flat-tops. Within a certain range of material coverage, the surface contains both coherent and dislocated islands, showing an overall bimodal island-size distribution. The continued deposition on such surfaces leads to the pronounced growth of dislocated islands, whereas the sizes of the coherent islands change very little.

PACS number(s): 68.55.−a, 61.14.Hg, 81.15.Hi

The III-V nitrides continue to attract intensive interest due to their promises in optoelectronic applications.[1] By adjusting the indium (In) content x in $In_xGa_{1-x}N$ alloys, the energy band gap of the material can be tuned from 0.7 eV to 3.4 eV, so the band-edge emission covers the whole visible spectrum.[1,2] However, due to a large lattice mismatch (e.g., ~10% between InN and GaN), the epitaxial growth of InGaN on GaN has been difficult. The lattice mismatch strain leads to the Stranski-Krastanov (SK) growth mode, where three-dimensional (3D) islands nucleate following an initial two-dimensional (2D) wetting-layer formation. Depending on the amount of strain, the SK islands can be coherent to the lattice of the substrate, or they may be dislocated.[3,4] The driving force for the spontaneous formation of the 3D islands is to accommodate or relieve the strain in the system. The coherent islands of semiconductors have drawn special attention, as they may act as the "quantum dots" in modern optoelectronic and/or microelectronic devices.[5] In contrast to other semiconductor systems, the heteroepitaxial growth mode and island characteristics of nitrides remain poorly characterized so far.

In this paper, we follow the SK growth of the InGaN alloy on GaN(0001) during molecular-beam epitaxy (MBE). The newly nucleated islands are shown to be cone-shaped and coherent to the underlying GaN. As they grow bigger, the islands become dislocated. Over a range of material coverage, both coherent and dislocated islands exist on the same surface, showing an overall bimodal size distribution. In such situations, continued deposition results in the pronounced growth of the dislocated islands, whereas the small, coherent islands change little in size.

The experiments were conducted in a multichamber ultrahigh vacuum (UHV) system, where the MBE reactor and some surface analysis tools were connected via vacuum interlocks. In the MBE chamber, the effusion cells for gallium (Ga) and In were installed together with a radio-frequency (rf) plasma unit for nitrogen (N). Before depositing the InGaN alloy, a thick (≥ 1 μm) GaN layer was grown on $6H$-SiC(0001) at about 600 °C using an excess Ga flux,[6] which then acted as the pseudosubstrate for subsequent InGaN deposition at a lower temperature of 390 °C. The sample heating was achieved by flowing a direct current through the long side of the rectangular sample piece, and the temperature was measured by a focus infrared pyrometer. During the alloy deposition, the flux ratio between Ga and N was 0.3, while that between In and N was 0.9. The growth rate of the alloy was ~0.03 bilayers per second (BLs/s) according to the reflection high-energy electron-diffraction (RHEED) intensity oscillation measurements. The In composition x of the alloy was about 70% according to the measurements of the strain and the estimation from the source fluxes.[7,8] After depositing a nominal thickness of the film, the growth was stopped and the sample quenched by switching off the heating current. Then the surfaces were examined by scanning tunneling microscopy (STM) in an adjacent UHV chamber. A constant-current mode of STM was conducted at room temperature under a sample bias of −2.0 V and a tunneling current of 0.1 nA.

Figure 1 shows a set of STM images depicting the evolution of surfaces as the deposition of InGaN proceeds. At the nominal coverage of 2.1 bilayers (BLs), no 3D islands are observed [Fig. 1(a)]. Rather, the surface contains triangularly shaped 2D islands that are 1 BL high, suggesting the growth to be 2D nucleation at this stage. At the coverage of 2.5 BLs [Fig. 1(b)], the surface starts to show minute 3D islands, signifying the 2D to 3D transition and thus the SK growth mode. Upon depositing 3.3 BLs [Fig. 1(c)], the surface shows some large 3D islands in addition to the small ones. The densities of both large and small islands increases as the deposition continues [Fig. 1(d) for 7 BLs] until it reaches the aggregation regime, where the existing islands coarsen, and the overall density of the islands remains unchanged.
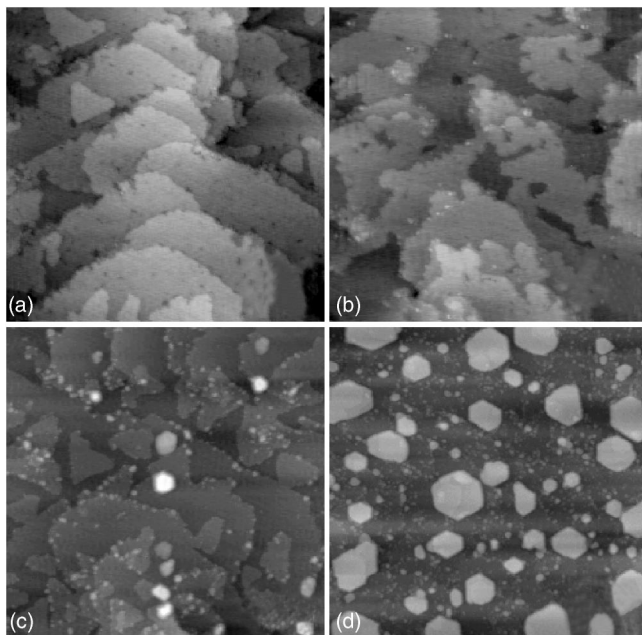
FIG. 1. STM images of surfaces following $In_xGa_{1-x}N$ deposition on GaN(0001) for the nominal thicknesses of (a) 2.1 BLs, (b) 2.5 BLs, (c) 3.3 BLs, and (d) 7.0 BLs. Image sizes: 200×200 nm^2 for (a)–(c) and 500×500 nm^2 for image (d).

The large and small islands identified above show distinctly different shapes, as illustrated by the line profiles in Fig. 2. The small islands are cone shaped with circular bases. On the other hand, the large islands are pillarlike, having flat tops. The bases of the large islands are predominantly hexagonal. A line-profile analysis of many of the islands does not suggest faceting for the cone-shaped islands. The data for the island aspect ratio [see Fig. 3(b) below] are very scattered, indicating the kinetic nature of the island shape selection. The pillar-shaped islands, on the other hand, are bounded by (0001) planes at the top. For the sidewalls, the STM measurements at different scan lengths and speeds indicate that they are likely vertical $\{11\bar{2}0\}$ and $\{10\bar{1}0\}$ planes, though the convoluted STM line profiles all show nonvertical edges. We further measured the island heights H and lateral sizes L, and the results are summarized in Figs. 3(a) and 3(b) for the height and aspect ratio H/L, respectively. From Fig. 3(a), one observes that for the cone-shaped islands, the height increases rapidly with increasing lateral

size, whereas for the pillar-shaped islands, the heights vary slowly with the lateral dimension. From Fig. 3(b), one notes that for the pillar-shaped islands, the aspect ratio decreases continuously with increasing lateral size, which is not obvious for the cone-shaped islands. All of these differences, we believe, reflect the very different characters of the two islands.

Previous studies on the characteristics of the SK islands showed that the island aspect ratio *increases* continuously with size for coherent and unfacetted islands.[9,10] For facetted islands, which is generally the case for crystalline semiconductors, the shape transition may take place at some critical size, above which island shapes with larger aspect ratios become favorable.[4,11–13] The latter was verified experimentally for Ge/Si and InAs/GaAs systems.[14,15] Therefore, the decreasing trend of the aspect ratio seen in Fig. 3(b) for the pillar-shaped InGaN islands is inconsistent with these previous investigations. However, in a recent study of the heteroepitaxial growth of binary InN on GaN(0001), a similar decreasing trend of island aspect ratio was reported.[16,17] In that case, the measurements of strain by *in situ* RHEED indicated a partial relaxation of the misfit strain by defects in the islands.[18] Taking this factor into account, a decreasing island aspect ratio with size is less surprising.[16] Indeed for such islands, the strain-relieving defects diminish the driving potential for the atoms' up-diffusion, and so the increase in the island height becomes gradually arrested. Based on this analysis, we infer that the cone-shaped InGaN islands, which are nucleated initially following the completion of the wetting layer, are coherent SK islands, whereas the large pillar-shaped islands are dislocated upon growing above a critical size (~ 20 nm in the lateral dimension).

While the dynamic and kinetic details of the island shape change from cones to pillarlike are unclear, the stagnation of the island height growth for the large dislocated islands is evident in Fig. 3(a). At this stage, continued growth in the lateral dimension naturally creates a plateau at the island top. A strong anisotropy in the growth rate sets in between the vertical and lateral directions. By measuring the island dimension following the deposition of different coverages, the degree of growth-rate anisotropy is estimated. The results show that the lateral growth is about 5 times faster than the growth in the vertical direction.

Lastly, Figs. 4(a) and 4(b) plot the size distributions of the islands following 10 and 13 BL materials deposition, respectively. For both coverages, the two types of islands coexist
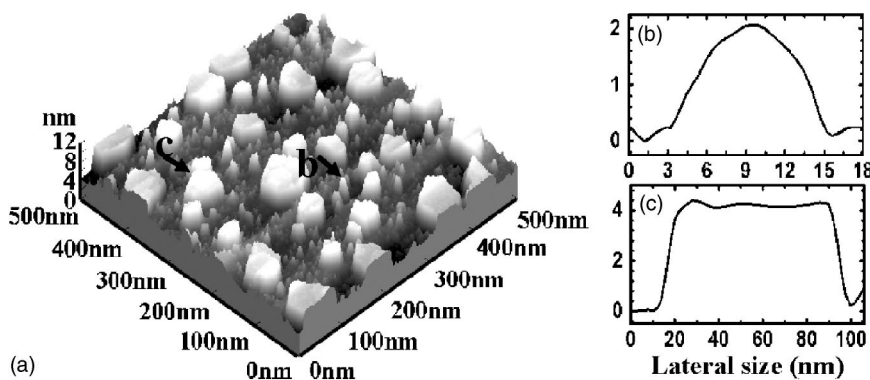

FIG. 2. (a) A prospective STM image showing 3D InGaN islands formed on GaN(0001). (b) and (c) are line profiles depicting the shape of small and large islands, respectively.
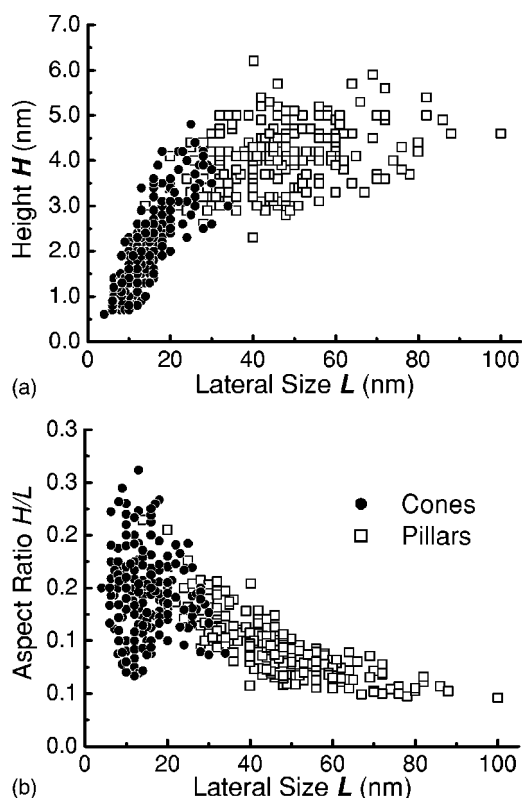
FIG. 3. (a) Island height H and (b) aspect ratio H/L, plotted as a function of the lateral dimension L.
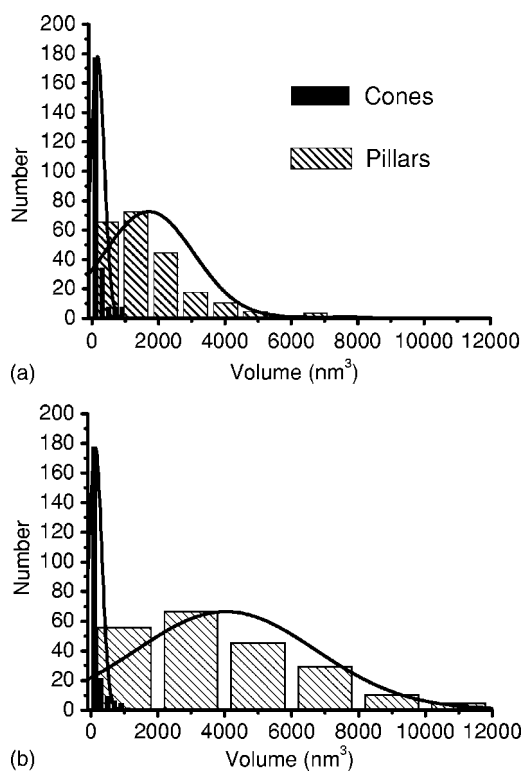

FIG. 4. Histograms showing the distribution of sizes for the cone-shaped and pillarlike islands following nominal (a) 10-BL and (b) 13-BL material deposition. The curves represent the Gaussian fits to the distributions.

on surfaces. From these distribution curves, one firstly reaffirms the vastly different sizes corresponding to the two island shapes. The overall size distributions are bimodal. Similar bimodal distribution curves have been recorded in other heteroepitaxial systems as well,[15,19,20] which were associated with the shape change of islands.[20,21] In our case, since the cone-shaped islands are coherent while the pillarlike islands are defected, the two islands show different growth rates. According to Refs. 22 and 23, if coherent and dislocated islands coexisted on the surface, the latter would grow faster than the former. This is understood by the fact that the growth of coherent islands leads to an increase of the strain energy; whereas for dislocated islands, since the lattice mismatch strain has been mostly relieved by defects, the growth of such islands will clearly be energetically preferred.[24] The result of Fig. 4, where the increase in material coverage has led to the significant growth of the pillar-shaped islands but little change for the cone-shaped islands, is consistent with this expectation.

To summarize, in the SK growth of $In_xGa_{1-x}N$ on

GaN(0001), the initial 3D islands are coherent, having a conical unfacetted shape. When they have grown to above a critical size (≥ 20 nm in lateral dimension), defects are introduced in the islands. The shape of the islands also changes to a pillarlike shape, developing flat tops. At this stage, a strong anisotropy in the growth rate in the lateral versus the vertical directions is noted, which gives rise to a decreased aspect ratio with an increasing island size. When both coherent and dislocated islands are present on the same surface, further deposition leads to the rapid growth of the dislocated islands, while the coherent islands remain little changed in size.

*Electronic address: mhxie@hkusua.hku.hk

[1] S. Strite and H. Morkoc, J. Vac. Sci. Technol. B **10**, 1237 (1992).

[2] A. G. Bhuiyan, A. Hashimoto, and A. Yamamoto, J. Appl. Phys. **94**, 2779 (2003).

[3] J. W. Matthews, D. C. Jackson, and A. Chambers, Thin Solid Films **26**, 129 (1975).

[4] C. Ratsch and A. Zangwill, Surf. Sci. **293**, 123 (1993).

[5] D. Bimberg, M. Grundmann, and N. N. Ledentsov, *Quantum Dot Heterostructures* (John Wiley & Sons, Chichester, UK, 1999).

[6] S. M. Sean, M. H. Xie, W. K. Zhu, L. X. Zheng, H. S. Wu, and S.

Y. Tong, Surf. Sci. **445**, L71 (2000).

[7] Y. Liu, Y. G. Cao, H. S. Wu, M. H. Xie, and S. Y. Tong, J. Appl. Phys. **97**, 023502 (2005).

[8] T. Böttcher, S. S. Einfeldt, V. Kirchner, S. Figge, H. Heinke, D. Hommel, H. Selke, and P. L. Ryder, Appl. Phys. Lett. **73**, 3232 (1998).

[9] H. T. Johnson and L. B. Freund, J. Appl. Phys. **81**, 6081 (1997).

[10] B. J. Spencer and J. Tersoff, Phys. Rev. Lett. **79**, 4858 (1997).

[11] L. G. Wang, P. Kratzer, N. Moll, and M. Scheffler, Phys. Rev. B **62**, 1897 (2000).

[12] I. Daruka, J. Tersoff, and A.-L. Barabási, Phys. Rev. Lett. **82**, 2753 (1999).

[13] J. Tersoff and R. M. Tromp, Phys. Rev. Lett. **70**, 2782 (1993).

[14] H. Saito, K. Nishi, and S. Sugou, Appl. Phys. Lett. **74**, 1224 (1999).

[15] G. Medeiros-Ribeiro, A. M. Bratkovski, T. I. Kamins, D. A. A. Ohlberg, and R. S. Williams, Science **279**, 353 (1998).

[16] Y. G. Cao, M. H. Xie, Y. Liu, Y. F. Ng, H. S. Wu, and S. Y. Tong, Appl. Phys. Lett. **83**, 5157 (2003).

[17] Y. G. Cao, M. H. Xie, Y. Liu, S. H. Xu, Y. F. Ng, H. S. Wu, and S. Y. Tong, Phys. Rev. B **68**, 161304(R) (2003).

[18] Y. F. Ng, Y. G. Cao, M. H. Xie, X. L. Wang, and S. Y. Tong, Appl. Phys. Lett. **81**, 3960 (2002).

[19] S. Anders, C. S. Kim, B. Klein, M. W. Keller, R. P. Mirin, and A. G. Norman, Phys. Rev. B **66**, 125309 (2002).

[20] F. M. Ross, J. Tersoff, and R. M. Tromp, Phys. Rev. Lett. **80**, 984 (1998).

[21] R. E. Rudd, G. A. D. Briggs, A. P. Sutton, G. Medeiros-Ribeiro, and R. S. Williams, Phys. Rev. Lett. **90**, 146101 (2003).

[22] M. Krishnamurthy, J. S. Drucker, and J. A. Venables, J. Appl. Phys. **69**, 6461 (1991).

[23] J. Drucker, Phys. Rev. B **48**, 18 203 (1993).

[24] S. C. Jain, J. R. Willis, and R. Bullough, Adv. Phys. **39**, 127 (1990).